

# Reactions of Ester Derivatives of Carcinogenic *N*-(4-Biphenyl)hydroxylamine and the Corresponding Hydroxamic Acid with Purine Nucleosides

Sonya A. Kennedy, Michael Novak,\* and Brent A. Kolb

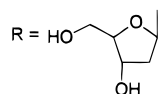
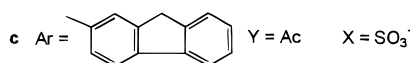
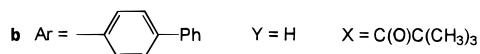
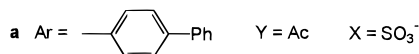
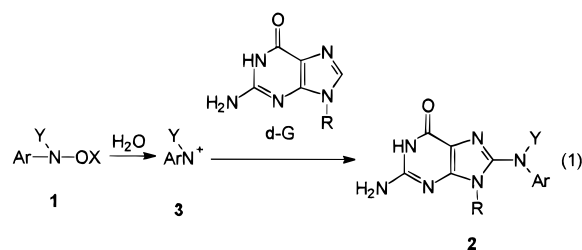
Contribution from the Department of Chemistry and Biochemistry, Miami University, Oxford, Ohio 45056

Received March 4, 1997<sup>⊗</sup>

**Abstract:** The nitrenium ions **3a,b** derived from hydrolysis of *N*-(sulfonatoxy)-*N*-acetyl-4-aminobiphenyl (**1a**) and *N*-(4-biphenyl)-*O*-pivaloylhydroxylamine (**1b**) are trapped by the purine nucleosides 2'-deoxyguanosine (dG), guanosine (G), 8-methylguanosine (8-MeG), adenosine (A), inosine (I), and xanthosine (X) with varying degrees of efficiency. Those nucleosides with a basic N-7 ( $\text{p}K_{\text{a}}(\text{N}^7\text{-H}^+) \geq 2.3$ ) react with **3a,b** with an apparently diffusion-limited rate constant at 20 °C of ca.  $2.0 \times 10^9 \text{ M}^{-1} \text{ s}^{-1}$ , determined from the experimental trapping ratios  $k_{\text{nuc}}/k_{\text{s}}$  and known values of  $k_{\text{s}}$  for the two nitrenium ions. All nucleosides with a basic N-7, including 8-MeG, generate only C-8 adducts upon reaction with **3a,b**. The reactions of 8-MeG with **3a,b** produce metastable adducts, tentatively identified as **16a,b**, that decompose over time into the stable 7,8-dihydroguanosine derivatives **8a,b**. Our data, and those of other workers, are consistent with a mechanism that involves initial attack of N-7 on the nitrogen of the nitrenium ions followed by a 1,2 migration and deprotonation (Scheme 2b) to yield the final C-8 adducts. Nucleosides with a less basic N-7 react more slowly with the nitrenium ions and also produce adducts other than C-8 adducts. Inosine generates both the C-8 adducts **6a,b** and the O-6 adducts **7a,b**. Adenosine reacts with **3a,b** to produce the unique azabicyclo[4.1.0]hepta-2,4-diene derivatives **11a,b**. Plots of  $\log k_{\text{nuc}}$  vs  $\text{p}K_{\text{a}}(\text{N}^7\text{-H}^+)$  show that the  $\beta_{\text{nuc}}$  for C-8 adduct formation is at least 0.7 for purine nucleosides with  $\text{p}K_{\text{a}} \leq 2.3$ . The purine and pyrimidine selectivity data conclusively demonstrate that the high abundance of C-8 dG adducts observed in DNA from in vivo or in vitro experiments is a consequence of the high selectivity of nitrenium ions for N-7 of dG. Other minor DNA adducts may be produced as a result of structure-dependent modification of site selectivity.

## Introduction

The carcinogenic esters, **1**, react with DNA, DNA oligomers, mononucleotides, and mononucleosides predominantly at the guanosine base to produce the C-8 adduct, **2**, as the major carcinogen–nucleic acid adduct (eq 1).<sup>1,2</sup> We recently showed



that **1a,c** react with 2'-deoxyguanosine (dG) to produce **2a,c**

via nucleophilic trapping of the diffusionally equilibrated nitrenium ions **3a,c** generated by rate-limiting N–O bond heterolysis (eq 1).<sup>3</sup> Kadlubar and co-workers have shown that the reaction occurs by nucleophilic attack of N-7 of dG on the nitrenium ion followed by rearrangement to form the C-8 adduct, but the detailed mechanism of this reaction has remained unclear.<sup>4</sup> Although guanosine is the major site of reaction in vitro and in vivo, it is known that other purines and pyrimidines react to form minor adducts.<sup>5</sup> In particular, it has been reported that adenosine also forms a C-8 adduct, but no confirming structural data have been published.<sup>5a–c</sup>

The mechanisms of these reactions are poorly understood, and the identities of minor adducts formed with bases other than guanosine are largely unknown. For this reason, we initiated a study of the reactions of the two ester derivatives of *N*-(4-biphenyl)hydroxylamine (**1a,b**) with the purines dG, guanosine (G), 8-methylguanosine (8-MeG), adenosine (A), inosine (I),

(1) (a) Kriek, E. *Chem.-Biol. Interact.* **1969**, *1*, 3–17. (b) Kriek, E. *Chem.-Biol. Interact.* **1971**, *3*, 19–28. (c) Meerman, J. H. N.; Beland, F. A.; Mulder, G. J. *Carcinogenesis* **1981**, *2*, 413–416. (d) Fuchs, R. P. P. *Anal. Biochem.* **1978**, *91*, 663–673. (e) Beland, F. A.; Dooley, K. L.; Jackson, C. D. *Cancer Res.* **1982**, *42*, 1348–1354. (f) Tamura, N.; King, C. M. *Carcinogenesis* **1990**, *11*, 535–540. (g) Kriek, E.; Miller, J. A.; Juhl, U.; Miller, E. C. *Biochemistry* **1967**, *6*, 177–182. (h) Nelson, J. H.; Grunberger, D.; Cantor, C. R.; Weinstein, I. B. *J. Mol. Biol.* **1971**, *62*, 331–346. (i) Evans, F. E.; Miller, D. W.; Levine, R. A. *J. Am. Chem. Soc.* **1984**, *106*, 396–401.

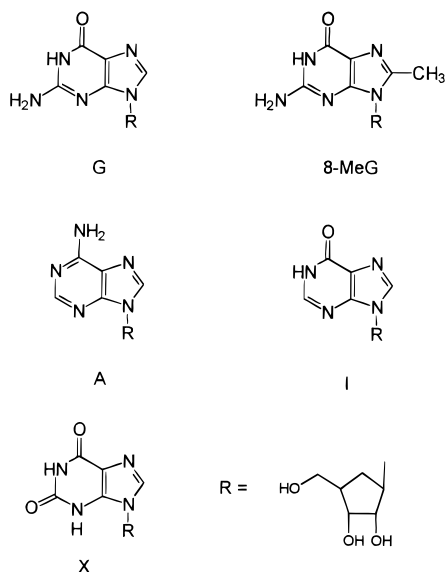
(2) Underwood, G. R.; Price, M. F.; Shapiro, R. *Carcinogenesis* **1988**, *9*, 1817–1821. Lee, M.-S.; King, C. M. *Chem.-Biol. Interact.* **1981**, *34*, 239–248. Van de Poll, M. L. M.; Van der Hulst, D. A. M.; Tate, A. D.; Meerman, J. *Carcinogenesis* **1990**, *11*, 333–339. Shapiro, R.; Underwood, G. R.; Zawadzka, H.; Broyde, S.; Hingerty, B. *Biochemistry* **1986**, *25*, 2198–2205.

(3) Novak, M.; Kennedy, S. A. *J. Am. Chem. Soc.* **1995**, *117*, 574–575.

(4) Humphreys, W. G.; Kadlubar, F. F.; Guengerich, F. P. *Proc. Natl. Acad. Sci. U.S.A.* **1992**, *89*, 8278–8282.

<sup>⊗</sup> Abstract published in *Advance ACS Abstracts*, August 1, 1997.

and xanthosine (X) in aqueous solution. Herein, we report the



structures of all significant adducts of these nucleosides with **1a,b** and we provide detailed mechanisms for these reactions based on the results of kinetic studies, nucleoside–solvent competition experiments, and the identification of metastable reaction intermediates. Our data provide a relatively complete picture of the factors that govern the nature of the purine–carcinogen reaction for carcinogens that generate long-lived nitrenium ions.

## Experimental Section

All reactions were performed in 5 vol %  $\text{CH}_3\text{CN}-\text{H}_2\text{O}$ ,  $\mu = 0.5$  ( $\text{NaClO}_4$ ), buffered with 20 mM phosphate or acetate buffers. Methods for purification of solvents, preparation of buffers, and handling of kinetic and product study data have been published.<sup>3,6,7</sup> All nucleosides except 8-MeG were obtained commercially and were used without further purification.

### Kinetic Studies:

Reaction kinetics for **1a** or **1b** in the presence and absence of purines were monitored by HPLC with UV detection at 250 or 260 nm or by UV spectroscopy at 306 or 310 nm. HPLC conditions were as follows: C-8 Ultrasphere octyl column, 3/2 or 1/1 MeOH/ $\text{H}_2\text{O}$  buffered with 1/1 NaOAc/HOAc, 0.05 M total buffer, 1 mL/min. An initial concentration of  $1.0 \times 10^{-4}$  M or  $5 \times 10^{-5}$  M in **1a** or **1b** was obtained by injection of 15  $\mu\text{L}$  of a 20 or 10 mM stock in DMF (**1a**) or  $\text{CH}_3\text{CN}$  (**1b**) into 3 mL of nucleoside solution ranging from 5 to 60 mM. Reactions were monitored at 20 °C for **1a** and 0 °C for **1b**. Rate constants were determined at pH 7.5 (9/1  $\text{Na}_2\text{HPO}_4/\text{NaH}_2\text{PO}_4$ ), pH 6.6 (1/1  $\text{Na}_2\text{HPO}_4/\text{NaH}_2\text{PO}_4$ ), pH 5.6 (9/1 NaOAc/HOAc), pH 4.6 (1/1 NaOAc/HOAc), and pH 3.6 (1/9 NaOAc/HOAc).

**Product Studies.** Product yields for **1a,b**, at an initial concentration of  $1.0 \times 10^{-4}$  M, were determined at 20 °C in purine and pyrimidine solutions ranging from 1 mM to 0.4 M. Buffers were prepared as described above. Yields were determined by triplicate HPLC injections on a  $\mu$ -Bondapak C-18 or C-8 Ultrasphere octyl column using the solvent and detector conditions described above.

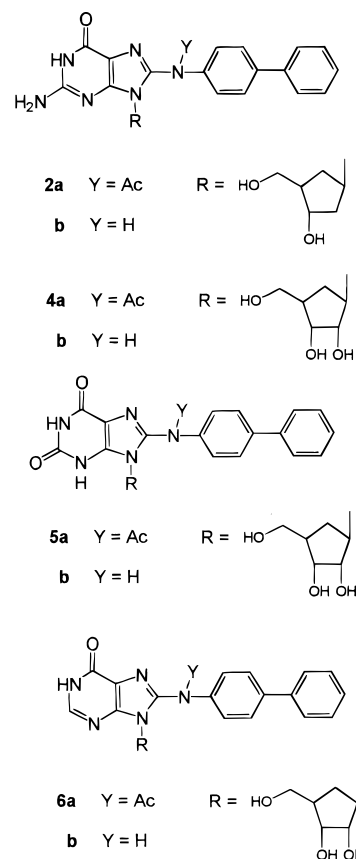
(5) (a) Beland, F. A.; Kadlubar, F. F. *Environ. Health Perspect.* **1985**, *62*, 19–30. (b) Beland, F. A.; Kadlubar, F. F. In *Chemical Carcinogenesis and Mutagenesis I*; Cooper, C. S., Grover, P. L., Eds.; Springer-Verlag: Berlin, 1990; pp 267–326. (c) Swaminathan, S.; Frederickson, S. M.; Hatcher, J. F. *Carcinogenesis* **1994**, *14*, 611–617. (d) Scribner, J. D.; Smith, P. L.; McCloskey, J. A. *J. Org. Chem.* **1978**, *43*, 2085–2087. (e) Scribner, J. D.; Naimy, N. K. *Cancer Res.* **1975**, *35*, 1416–1421.

(6) Novak, M.; Pelecanou, M.; Roy, A. K.; Andronico, A. F.; Plourde, F. M.; Olefirowicz, T. M.; Curtin, T. J. *J. Am. Chem. Soc.* **1984**, *106*, 5623–5631.

(7) Novak, M.; Kahley, M. J.; Eiger, E.; Helmick, J. S.; Peters, H. E. *J. Am. Chem. Soc.* **1993**, *115*, 9453–9460.

**NMR Studies of 1b with 8-MeG.** The decomposition of **1b** in deuterated 8-MeG solution (8.0 mM, 25%  $\text{DMF-}d_7/\text{D}_2\text{O}$ , 20 mM 9/1  $\text{Na}_2\text{DPO}_4/\text{NaD}_2\text{PO}_4$ ) and phosphate buffer (20 mM, 9/1  $\text{Na}_2\text{DPO}_4/\text{NaD}_2\text{PO}_4$ ) at 0 °C was monitored on a 300 MHz NMR. Deuterated 8-MeG solutions and phosphate buffers were prepared by dissolving the appropriate buffer components in  $\text{D}_2\text{O}$ , lyophilizing the solutions, dissolving in  $\text{D}_2\text{O}$  again, lyophilizing again, and finally reconstituting with the appropriate volume of  $\text{D}_2\text{O}$  and  $\text{DMF-}d_7$ . An initial concentration of  $2.0 \times 10^{-3}$  M was obtained by 10  $\mu\text{L}$  injection of a 0.10 M solution of **1b** into 0.5 mL of the buffer.

**Synthesis and Product Isolation.** The syntheses of **1a,b** and the isolation and characterization of **2a,b** and **4b** have been described.<sup>2,3,8</sup>



8-MeG was synthesized by a modification of a known procedure.<sup>9</sup> That synthesis, and the isolation and characterization of all new carcinogen–nucleoside adducts, is described in the Supporting Information. 4-Aminobiphenyl (**15**) and *N*-acetyl-4-aminobiphenyl (**10**) were identified by comparison to authentic samples.<sup>10</sup>

## Results

**Structures of Purine–Carcinogen Adducts.** Both **1a,b** generate adducts with all the purine nucleosides under the aqueous conditions employed in this study (5 vol %  $\text{CH}_3\text{CN}-\text{H}_2\text{O}$ ,  $\mu = 0.5$  ( $\text{NaClO}_4$ ), pH 4.0–7.5, 20 °C). The nucleosides dG, G, and X<sup>−</sup> react with **1a,b** to form the C-8 adducts **2**, **4**, and **5** as the exclusive nucleoside–carcinogen adducts isolated. Minor products ( $\leq 2\%$  of the yield of the major C-8 adduct) may have escaped detection. I also reacts to form the C-8 adducts **6**, but the adducts **7** are also isolated as major products. The adducts **2a,b** and **4b** were identified by comparison to

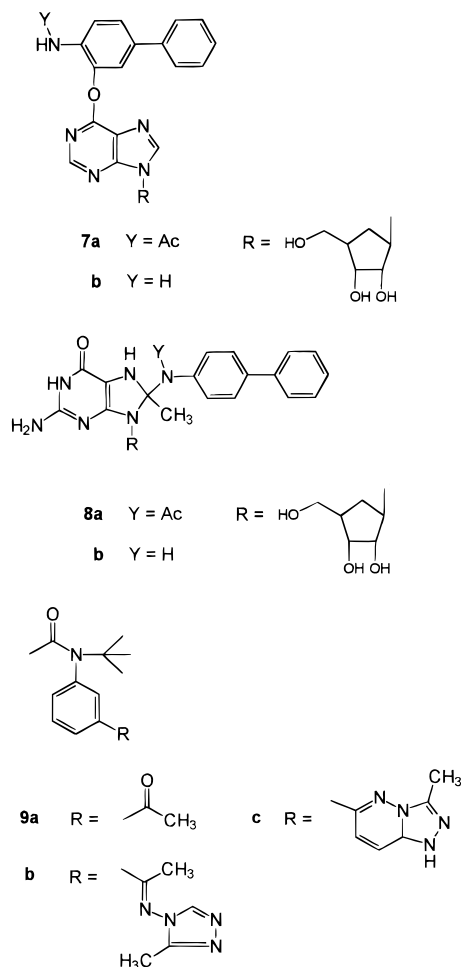
(8) Helmick, J. S.; Martin, K. A.; Heinrich, J. L.; Novak, M. *J. Am. Chem. Soc.* **1991**, *113*, 3459–3466. Novak, M.; Helmick, J. S.; Oberlies, N.; Rangappa, K. S.; Clark, W. M.; Swenton, J. S. *J. Org. Chem.* **1993**, *58*, 867–878.

(9) Maeda, M.; Nushi, K.; Kawazoe, Y. *Tetrahedron* **1974**, *30*, 2677–2682.

(10) Hazlet, S. E.; Dornfeld, C. A. *J. Am. Chem. Soc.* **1944**, *66*, 1781–1782.

published NMR data.<sup>2</sup> All C-8 adducts were identified by the disappearance in the <sup>1</sup>H NMR of the characteristic singlet for the purine C<sup>8</sup>-H and in the <sup>13</sup>C NMR by the replacement of the resonance for the tertiary C-8 with a resonance for a quaternary carbon. <sup>1</sup>H and <sup>13</sup>C NMR confirmed the absence of substitution at the tertiary aromatic carbons of the biphenyl systems.

For **1**, **7a** and **7b** represent 90% and 50%, respectively, of



the nucleoside-carcinogen adducts isolated. In **7a,b**, the <sup>1</sup>H and <sup>13</sup>C NMR resonances of the biphenyl systems are consistent with 1,2,4-trisubstitution in one of the aromatic rings. The <sup>1</sup>H and tertiary <sup>13</sup>C resonances for C<sup>2</sup>-H and C<sup>8</sup>-H of the purines are present, and the assignment of <sup>13</sup>C resonances in the purine rings of **7a,b** is consistent with the assignment previously made for *O*<sup>6</sup>-methylinosine (Figure 1).<sup>11</sup> Rotation about the *O*<sup>6</sup>-ether linkage is apparently hindered. At room temperature in DMSO-*d*<sub>6</sub>, the <sup>1</sup>H resonances for C<sup>2</sup>-H and C<sup>8</sup>-H for both compounds appear as closely spaced doublets. These coalesce into singlets above 70 °C. Some <sup>13</sup>C resonances in both compounds also show temperature-dependent coalescence behavior (see Supporting Information).

The adducts **2** and **4–7** are formed with no detectable intermediates, but the reactions of **1a,b** with 8-MeG are not as apparently simple. The isolated adducts are generated after the decomposition of metastable intermediates with *t*<sub>1/2</sub> at 20 °C of ca. 16 h for **1a** and ca. 5 h for **1b** (see below). In both cases, the isolated adducts consist of two diastereomers, produced in nearly equivalent yields, that can be separated from each other by reverse phase semipreparatory HPLC on a C<sub>8</sub> column. The

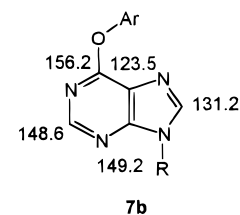
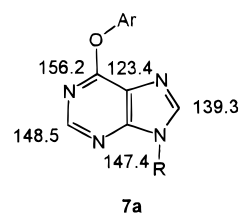
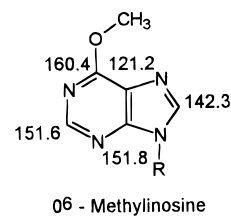


**Figure 1.** Comparison of <sup>13</sup>C NMR assignments for the purine rings of **7a,b** with those for *O*<sup>6</sup>-methylinosine.<sup>11</sup> All measurements were made in DMSO-*d*<sub>6</sub>.

structures assigned to these compounds on the basis of spectroscopic data are **8a,b**. In these compounds a new chiral center (C-8 of the dihydropurine) has been generated. This explains the presence of two diastereomeric products since 8-MeG is already chiral due to the ribose moiety. All four compounds were fully characterized by <sup>1</sup>H and <sup>13</sup>C NMR with complete COSY and XHCORR analysis for one member of each diastereomeric pair.

In all four compounds the ribose and 4-aminobiphenyl moieties are intact. The only possible point of attachment of the biphenyl system to the dihydropurine is through the 4-amino nitrogen. In the **8b** diastereomeric pair, the <sup>13</sup>C resonance of the quaternary C-8 carbon moves from 144.7 ppm in 8-MeG to 81.3 and 81.4 ppm in each diastereomer while the <sup>1</sup>H and <sup>13</sup>C resonances for the C<sup>8</sup>-CH<sub>3</sub> group move from 2.37 and 14.6 ppm, respectively, in 8-MeG to 1.22 and 29.0 ppm, respectively, in each diastereomer. In the **8a** pair, the <sup>13</sup>C resonances for the quaternary C-8 carbon are at 99.4 and 99.5 ppm and the C<sup>8</sup>-CH<sub>3</sub> <sup>1</sup>H and <sup>13</sup>C resonances are found at 1.42 and 1.38 and 26.9 and 26.3 ppm, respectively. The acyl-methyl group in each diastereomer has an unusually high-field <sup>1</sup>H resonance at 1.68 and 1.65 ppm. These resonances appear to be anomalous, but a series of related *N*-*tert*-butyl-*N*-arylacetamides (**9**) show the same <sup>1</sup>H upfield shift with resonances between 1.76 and 1.66 ppm.<sup>12</sup> MM2 and AM1 calculations suggest that the bulky tertiary group bonded to nitrogen stabilizes conformers in which the acyl-methyl group is positioned above the aromatic ring, thus shielding the acyl-methyl protons. There are two tertiary <sup>13</sup>C resonances, assigned to the tertiary carbons of the proximal aromatic ring of the biphenyl system, at ca. 131.0 and 127.6 ppm in each diastereomer of **8a** that show evidence of hindered rotation about the N-C bond of the biphenyl system. These resonances appear as two singlets of equal intensity at 20 °C in DMSO-*d*<sub>6</sub> but coalesce into broad singlets at 40 °C. This behavior is not unexpected considering the sterically congested nature of the structure of **8a** in the vicinity of the quaternary C-8. <sup>1</sup>H and <sup>13</sup>C assignments for one of the **8a** diastereomers are provided in Figure 2.

Although the **8b** diastereomers are indefinitely stable in neutral aqueous media, the **8a** diastereomers decompose slowly in aqueous solution at pH 7 (about 2 weeks at 50 °C) into *N*-acetyl-4-aminobiphenyl (**10**) and 8-MeG. These sterically hindered dihydropurines appear to be subject to a slow elimination process driven by relief of steric strain.

(11) Chenon, M.-T.; Pugmire, R. J.; Grant, D. M.; Panzica, R. P.; Townsend, L. B. *J. Am. Chem. Soc.* **1975**, *97*, 4627–4636.

(12) Albright, J. D.; Lieberman, D. F. *J. Heterocycl. Chem.* **1994**, *31*, 537–539.

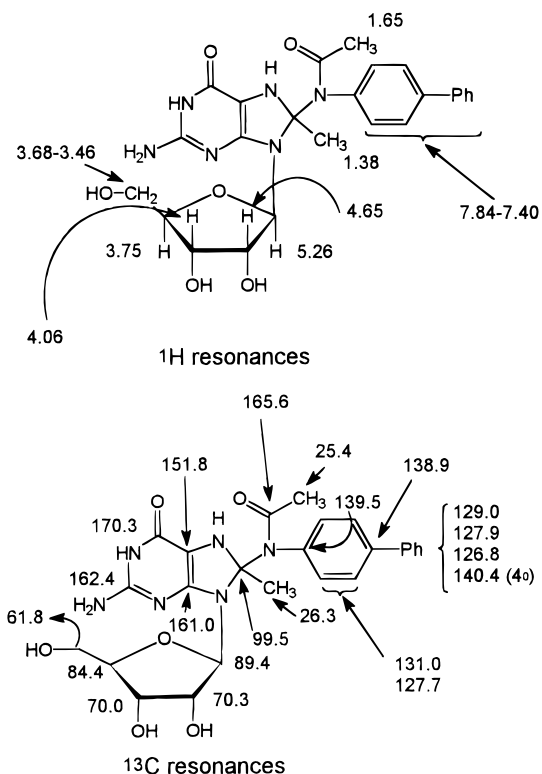
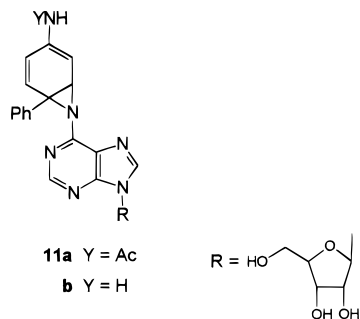
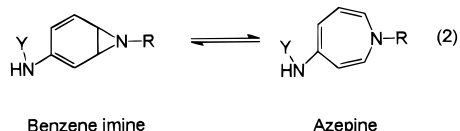


**Figure 2.**  $^1\text{H}$  and  $^{13}\text{C}$  NMR assignments for one diastereomer of **8a**.  $^1\text{H}$  assignments are made only for nonexchangeable protons.  $^{13}\text{C}$  assignments of some quaternary carbons are tentative.

The reactions of **1a,b** with **A** do not generate detectable C-8 adducts. In both cases, the only adducts isolated are the 7-azabicyclo[4.1.0]hepta-2,4-diene derivatives **11a,b**. Structural as-



signments are based on  $^1\text{H}$  and  $^{13}\text{C}$  NMR resonances and COSY and XHCORR assignments. Complete  $^1\text{H}$  and  $^{13}\text{C}$  assignments for **11a** are shown in Figure 3. These assignments are consistent with the azabicycloheptadiene (benzene imine) structure, not with the isomeric azepine structure (eq 2).



imines, the  $^{13}\text{C}$  resonances for C-1 and C-6 are found between 65 and 53 ppm, while the analogous  $^{13}\text{C}$  resonances in azepines are found around 150–130 ppm.<sup>13</sup> The  $^{13}\text{C}$  resonances assigned to the bridgehead carbons in **11a** are found at 62.9 (CH) and 72.6 (C) ppm. In **11b** these resonances are found at 64.4 (CH) and 72.4 (C) ppm.

(13) (a) Lange, W.; Tückmantel, W. *Chem. Ber.* **1989**, *122*, 1765–1776. (b) Vogel, E.; Altenbach, H.-J.; Drossard, J.-M.; Schmickler, H.; Stegelmeier, H. *Angew. Chem., Int. Ed. Engl.* **1980**, *19*, 1016–1018.

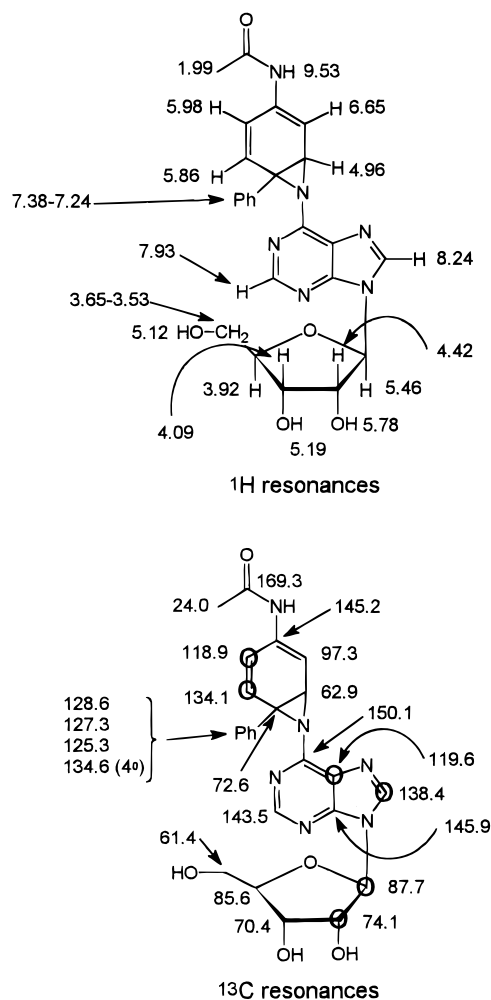


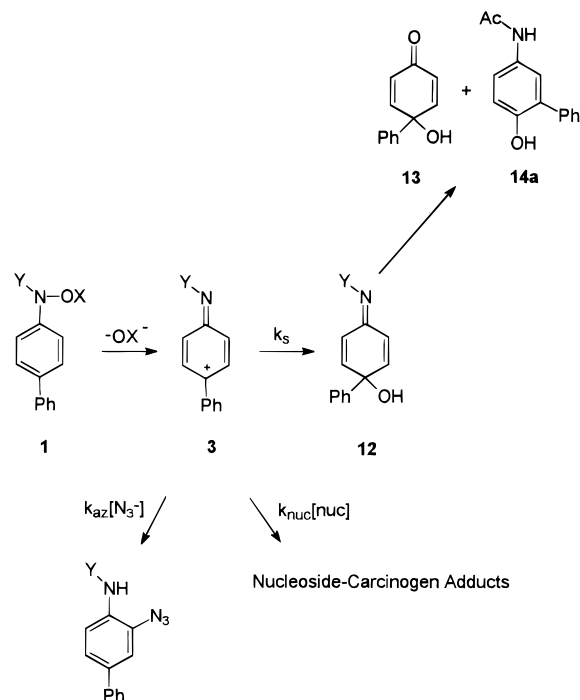
**Figure 3.**  $^1\text{H}$  and  $^{13}\text{C}$  assignments for **11a**.  $^{13}\text{C}$  assignments for some quaternary carbons are tentative.  $^{13}\text{C}$  resonances showing temperature-dependent coalescence are circled.

Although the NMR chemical shift data show that **11a,b** are benzene imine derivatives, there is evidence of a dynamic equilibrium between these materials and the isomeric azepines. Both **11a,b** should be produced as a pair of diastereomers, but we could find no HPLC conditions under which diastereomers were separated and no evidence in the  $^1\text{H}$  NMR of either compound for the presence of two diastereomers. This leads to the unlikely conclusion that **11a,b** consist of only a single diastereomer or, more likely, that the two diastereomers of **11a,b** are in rapid dynamic equilibrium. Previous attempts to probe the benzene imine  $\rightleftharpoons$  azepine equilibrium by dynamic NMR methods have failed even in equilibrium mixtures in which significant quantities of both isomers are present.<sup>13a</sup> This led to the conclusion that  $E_a$  for the isomerization reaction is less than 5 kcal/mol in  $\text{CDCl}_3$ .<sup>13a</sup>

The  $^{13}\text{C}$  NMR spectra of **11a,b** show several resonances (six for **11a** and five for **11b**) that appear as two singlets of equal intensity in  $\text{DMSO}-d_6$  at room temperature. These coalesce into singlets at higher temperatures. This behavior may be associated with a dynamic equilibrium between the two diastereomers of **11a,b**, but considering the previously unsuccessful attempts to observe the process by NMR, it is more likely that the temperature-dependent  $^{13}\text{C}$  NMR spectra of **11a,b** are due to hindered rotation about the purine C<sup>6</sup>–N bond. This is similar to the explanation given for the temperature-dependent NMR spectra of **7a,b**.

**Kinetics and Selectivity Ratios.** We have shown that **1a,b** undergo hydrolysis by rate-limiting heterolytic cleavage of the

## Scheme 1



N–O bond to form the diffusively equilibrated nitrenium ions **3a,b** (Scheme 1).<sup>7</sup> In the absence of other nucleophiles, **3a,b** are trapped by H<sub>2</sub>O to form the detectable quinol imines **12a,b** that subsequently decompose to form the major stable hydrolysis products **13** and **14a** from **12a** and **13** from **12b**.<sup>7</sup> The nitrenium ions are efficiently trapped by N<sub>3</sub><sup>−</sup> with  $k_{\text{az}}/k_s$  (Scheme 1), measured from product ratios, of  $1.0 \times 10^3 \text{ M}^{-1}$  for **3a** and  $2.9 \times 10^3 \text{ M}^{-1}$  for **3b**.<sup>7</sup> If  $k_{\text{az}}$  is assumed to be diffusion-limited at ca.  $5 \times 10^9 \text{ M}^{-1} \text{ s}^{-1}$ ,  $k_s$  can be estimated for both ions. These estimates are in excellent agreement with the directly measured  $k_s$  of  $5.9 \times 10^6 \text{ s}^{-1}$  for **3a** and  $1.8 \times 10^6 \text{ s}^{-1}$  for **3b** subsequently measured by McClelland and co-workers for the ions generated by laser flash photolysis under the same solvent conditions.<sup>14</sup>

The data in Table 1 show that the hydrolysis rate constants,  $k_o$ , for **1a,b** are independent of nucleoside concentrations under conditions in which the nucleoside–carcinogen adducts account for 40–90% of reaction products derived from the carcinogens. These results are similar to those previously observed for the small anionic nucleophiles N<sub>3</sub><sup>−</sup> and Cl<sup>−</sup>.<sup>7</sup>

Selectivity ratios,  $k_{\text{nuc}}/k_s$ , (Scheme 1), for the nucleosides can be determined from product distribution data as previously described for N<sub>3</sub><sup>−</sup> and dG.<sup>3,7,15</sup> Typical product vs nucleoside concentration data for the reaction of I with **1b** are shown in Figure 4. Other representative trapping data are shown in Figures S1–S6 in the Supporting Information. Observed selectivity ratios are gathered in Table 2. Combined yields of hydrolysis products and nucleoside–carcinogen adducts, determined from HPLC data, account for  $\geq 90\%$  of initial **1a** or **1b** except in X solutions at pH < 6.0. Selectivity ratios are pH independent in the pH range from 4.0 to 7.5 for all of the purine nucleosides except X. This occurs because this nucleo-

(14) (a) Davidse, P. A.; Kahley, M. J.; McClelland, R. A.; Novak, M. J. *Am. Chem. Soc.* **1994**, *116*, 4513–4514. (b) McClelland, R. A.; Davidse, P. A.; Hadzialic, G. *J. Am. Chem. Soc.* **1995**, *117*, 4173–4174.

(15) Selectivity ratios  $k_{\text{nuc}}/k_s$  were determined from yield data by a weighted nonlinear least-squares fit to % yield =  $(k_{\text{nuc}}/k_s)[\text{nuc}]/(1 + (k_{\text{nuc}}/k_s)[\text{nuc}])$  for nucleoside–carcinogen adducts. For hydrolysis products, the relationship used is % yield =  $1/(1 + (k_{\text{nuc}}/k_s)[\text{nuc}])$ . Values of  $k_{\text{nuc}}/k_s$  determined for different products in the same reaction were in good agreement ( $\pm 15\%$ ). Average values obtained from all products are reported in this paper.

**Table 1.** Hydrolysis Rate Constants for **1a,b** in the Presence of Purine Nucleosides

ester	conditions <sup>a</sup>	$k_o$ (s <sup>−1</sup> ) <sup>b</sup>	% trapping by nucleoside <sup>c</sup>
<b>1a</b>	no nucleoside	$(4.0 \pm 0.5) \times 10^{-4}$ <sup>d</sup>	
<b>1b</b>	no nucleoside	$0.12 \pm 0.01$ <sup>e</sup>	
<b>1a</b>	dG, 10.8 mM	$(4.2 \pm 0.3) \times 10^{-4}$ <sup>f</sup>	77%
<b>1b</b>	dG, 5.0 mM	$0.11 \pm 0.01$ <sup>g</sup>	84%
<b>1a</b>	8-MeG, 10 mM	$(4.2 \pm 0.2) \times 10^{-4}$	74%
<b>1b</b>	8-MeG, 10 mM	$0.11 \pm 0.02$	91%
<b>1a</b>	A, 50 mM	$(3.8 \pm 0.2) \times 10^{-4}$	55%
<b>1b</b>	A, 40 mM	$0.090 \pm 0.004$	40%
<b>1a</b>	I, 60 mM	$(4.1 \pm 0.1) \times 10^{-4}$	65%
<b>1b</b>	I, 60 mM	$0.090 \pm 0.004$	80%
<b>1a</b>	X, 10 mM	$(4.0 \pm 0.2) \times 10^{-4}$	71%
<b>1b</b>	X, 10 mM	$0.093 \pm 0.003$	92%

<sup>a</sup> 5% CH<sub>3</sub>CN–H<sub>2</sub>O,  $\mu = 0.5$  (NaClO<sub>4</sub>), buffered with 20 mM acetate or phosphate buffers.  $T = 20$  °C for **1a** and 0 °C for **1b**. <sup>b</sup> For **1a** measured by HPLC monitoring of **1a** or reaction products. Initial concentration of **1a** =  $1.0 \times 10^{-4}$  M. For **1b** measured by UV spectroscopy at 305–310 nm. Initial concentration of **1b** =  $5 \times 10^{-5}$  M. Rate constants measured at pH 7.5 unless otherwise indicated. <sup>c</sup> As calculated from the data in Table 2. <sup>d</sup> Average value over pH range 1.0–9.0. See ref 7. <sup>e</sup> Average value over pH range 3.7–7.5 (this work and ref 7). <sup>f</sup> Average of three measurements made at pH 3.7, 4.5, and 7.5. <sup>g</sup> Average of five measurements made at pH 3.8, 4.6, 5.6, 6.7, and 7.4.

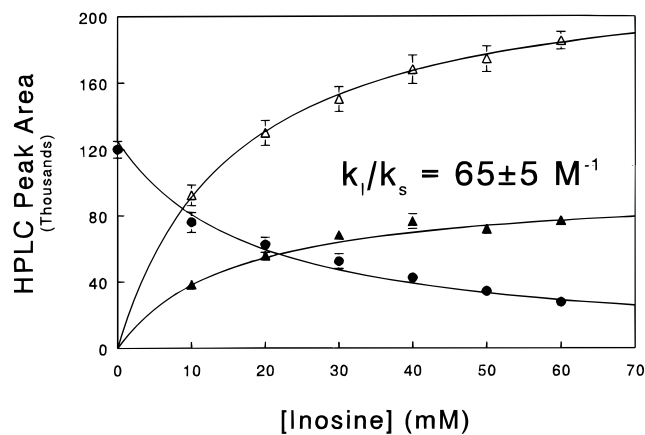


**Figure 4.** Plot of product yields vs nucleoside concentrations for the reaction of **1b** with inosine at pH 7.5: **12b** (●), **6b** (▲), **7b** (△). The theoretical lines were obtained as described in footnote 15.

side has a  $\text{p}K_a$  for N<sup>1</sup>–H at ca. 5.7.<sup>16</sup> Figure 5 shows a plot of observed  $k_X/k_s$  vs pH for **1a**. A similar plot for **1b** is shown in Figure S7 in the Supporting Information. The data were fit to a standard titration curve to obtain  $k_X/k_s$ ,  $k_X^-/k_s$ , and  $\text{p}K_a$  for X. The  $\text{p}K_a$ 's of  $5.60 \pm 0.05$  and  $5.65 \pm 0.05$  determined from the two fits are in good agreement with each other and with literature  $\text{p}K_a$  data.<sup>16</sup> The less than quantitative detection of products at low pH in X solutions indicates that additional nucleoside–carcinogen adducts may be formed at low pH, but these were not detected.

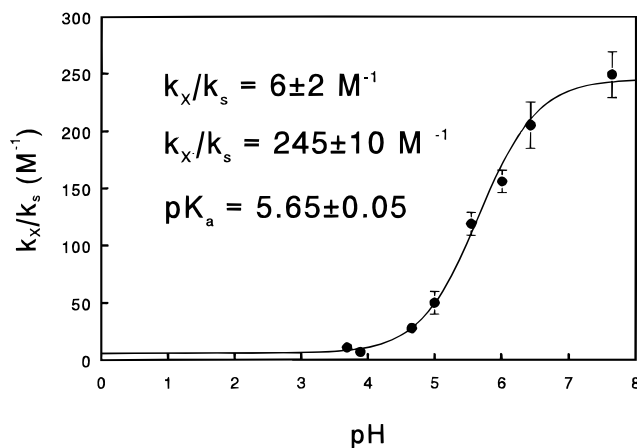
The selectivity ratios may measure the competition of the nucleoside and solvent for the nitrenium ions **3a,b**, or possibly for the quinol imines **12a,b**. Since **12a,b** are detectable species, these two alternatives can be distinguished by kinetic methods. Figure 6A shows that in the absence of nucleosides **12b**, generated from the rapid hydrolysis of **1b**, decomposes at pH 7.5 with a pseudo-first-order rate constant of  $(1.34 \pm 0.02) \times 10^{-4} \text{ s}^{-1}$  and **13** is formed with the same rate constant. Figure 6B shows that in the presence of 60 mM I the rate constants

(16) Dunn, D. B.; Hall, R. H. In *CRC Handbook of Biochemistry and Molecular Biology, Nucleic Acids*, 3rd ed.; Fasman, G. D., Ed.; CRC Press: Inc.; Cleveland, OH, 1975; Vol. 1, pp 65–215.

**Table 2.** Selectivity Ratios for Trapping of **3a,b** by Purine and Pyrimidine Nucleosides and H<sub>2</sub>O<sup>a</sup>

	selectivity ratios (M <sup>-1</sup> )	
	<b>3a</b>	<b>3b</b>
$k_{dG}/k_s$	314 ± 16 <sup>b</sup>	1060 ± 100
$k_G/k_s$	359 ± 11	680 ± 50
$k_{8-MeG}/k_s$	292 ± 12	1000 ± 100
$k_A/k_s$	24 ± 1	17 ± 1
$k_I/k_s$	31 ± 4	65 ± 5
$k_X/k_s$	6 ± 2	85 ± 15
$k_{X^-}/k_s$	245 ± 10	1200 ± 50
$k_T/k_s$	≤ 1.2 ± 0.1	≤ 4.3 ± 0.5
$k_U/k_s$	≤ 1.0 ± 0.2	
$k_C/k_s$	≤ 1.6 ± 0.4	

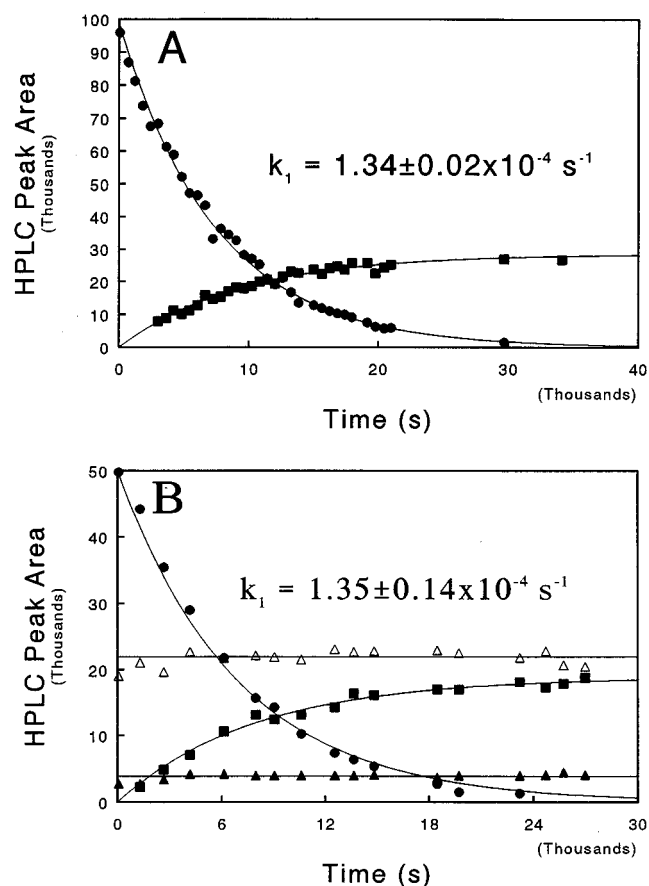
<sup>a</sup> Conditions for both **1a,b**: 5% CH<sub>3</sub>CN–H<sub>2</sub>O,  $\mu = 0.5$  (NaClO<sub>4</sub>), buffered with 20 mM acetate or phosphate buffers,  $T = 20$  °C, initial concentrations of **1a,b** =  $1.0 \times 10^{-4}$  M. <sup>b</sup> The previously reported value of 290 M<sup>-1</sup> was obtained at pH 7.5 (ref 3). This value is an average of four runs in the pH range 3.6–7.5.

**Figure 5.** Plot of observed  $k_X/k_s$  vs pH for **1a**. Data were fit to a standard titration curve by a weighted nonlinear least-squares method.

for disappearance of **12b** and appearance of **13** are not changed. The adducts **6b** and **7b** are formed rapidly before any significant hydrolysis of **12b** occurs, so their concentrations are effectively constant throughout the time course for the disappearance of **12b**. Similar results were obtained for all the purine nucleosides used in this study. It is clear that the nucleoside–carcinogen adducts are derived from trapping of the nitrenium ions, not their quinol imine hydrolysis products.

Table 2 also shows data for the selectivity ratios for trapping of the nitrenium ions by the pyrimidine nucleosides thymidine (T), uridine (U), and cytosine (C). The selectivity ratios were determined from the decrease in yields of the final hydrolysis products as a function of pyrimidine concentrations. No nucleoside–carcinogen adducts were isolated, nor was it demonstrated whether trapping occurs on the nitrenium ion or the quinol imine, so these ratios are upper limits for the trapping of **3a,b** by the pyrimidines. Since the selectivity ratios are so low, no further experiments with the pyrimidines were pursued.

Since  $k_s$  is known for **3a,b** under these reaction conditions,<sup>14</sup> it is possible to calculate  $k_{nuc}$  for the reaction of all the purine nucleosides with both nitrenium ions (Table 3). The rate constants approach an approximate limit of  $2 \times 10^9$  M<sup>-1</sup> s<sup>-1</sup> for reaction of both **3a,b** with dG, G, 8-MeG, and X<sup>-</sup>. For A, I, and X the rate constants are considerably smaller. These rate constants refer to formation of a C-8 adduct for dG, G, 8-MeG, and X<sup>-</sup>. Since C-8 adducts **6a,b** make up a measurable fraction of the nucleoside–carcinogen reaction products for I, it is possible to estimate the rate constant for formation of the C-8

**Figure 6.** Plots of HPLC peak areas vs time for the products of the decomposition of **1b** at pH 7.5 in the absence of nucleosides (A) or in the presence of 60 mM inosine (B). Product data that varied with time were fit to a standard first-order rate equation. For product data that did not vary with time, the lines shown are the average values of those data during the experiment. (A): **12b** (●), **13** (■). (B): **12b** (●), **13** (■), **6b** (▲), **7b** (△).**Table 3.** Calculated Rate Constants for Reaction of Purine Nucleosides with Nitrenium Ions **3a,b**

nucleoside	$pK_a(N^7-H^+)^a$	$k_{nuc}$ (M <sup>-1</sup> s <sup>-1</sup> )	
		for <b>3a</b>	for <b>3b</b>
8-MeG	3.3	$1.7 \times 10^9$	$1.8 \times 10^9$
dG	2.6	$1.9 \times 10^9$	$1.9 \times 10^9$
G	2.3	$2.1 \times 10^9$	$1.2 \times 10^9$
X <sup>-</sup>	2.1 <sup>b</sup>	$1.4 \times 10^9$	$2.2 \times 10^9$
I	1.4	$1.8 \times 10^8$	$1.2 \times 10^8$
(for C-8 adduct)		$1.8 \times 10^7$	$5.9 \times 10^7$
X	0	$3.5 \times 10^7$	$1.5 \times 10^8$
(for C-8 adduct)		$1.9 \times 10^7$	$3.0 \times 10^7$
A	-1.6	$1.4 \times 10^8$	$3.1 \times 10^7$
(for C-8 adduct)		$< 2.8 \times 10^6$	$< 6.1 \times 10^5$

<sup>a</sup> Measured at  $\mu = 1.0$ ,  $T = 25$  °C, or extrapolated to  $\mu = 1.0$  from lower ionic strength measurements. See ref 17. <sup>b</sup> Estimated. See ref 18.

adducts **6a,b**. These are included in Table 3. Table 3 also contains estimated rate constants for the formation of C-8 adducts from X, based on yields of **5a,b** at low pH that indicate these products account for 55% and 20%, respectively, of the trapping reaction. Upper limits for rate constants for reaction of A with **3a,b** to produce C-8 adducts can be estimated from the approximate detection limit (ca. 2%) established for the formation of an adenosine C-8 adduct. These estimates are also included in Table 3.

Plots of  $\log k_{nuc}$  for the formation of C-8 adducts vs the  $pK_a$  of  $N^7-H^+$  for the purine nucleosides<sup>17</sup> are shown in Figure 7. For **3a,b**,  $k_{nuc}$  reaches a limit of ca.  $2 \times 10^9$  M<sup>-1</sup> s<sup>-1</sup> for  $pK_a \geq$

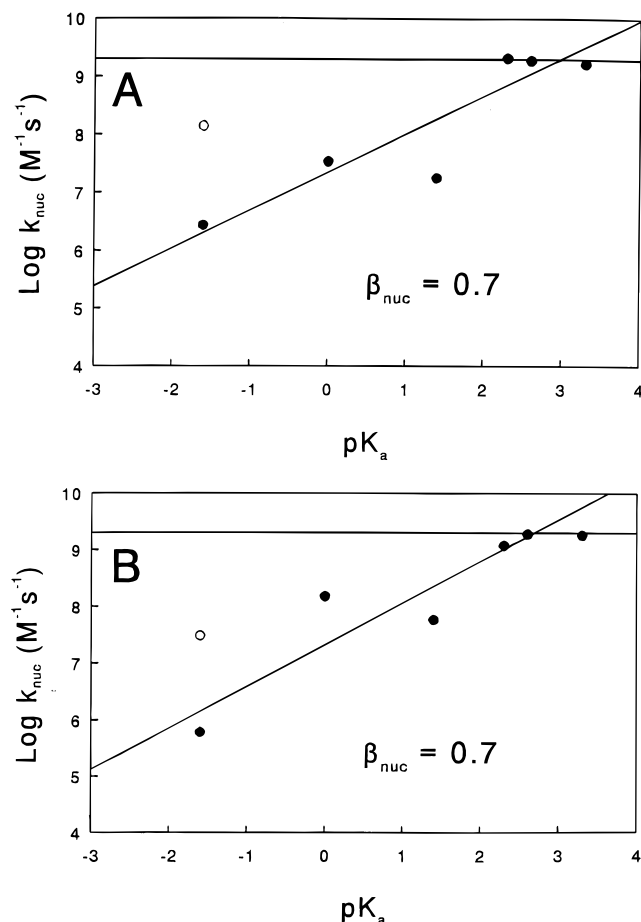


**Figure 7.** Log  $k_{\text{nuc}}$  for formation of C-8 adducts vs  $\text{pK}_a$  of  $\text{N}^7\text{-H}^+$  of the purine nucleosides for **3a** (A) and **3b** (B). Slopes,  $\beta_{\text{nuc}}$ , were estimated from a linear least-squares fit of the data for nucleosides with  $\text{pK}_a \leq 2.3$ . The estimated diffusion limit of  $2 \times 10^9 \text{ M}^{-1} \text{ s}^{-1}$  for  $k_{\text{nuc}}$  is shown in both plots. The data point for adenosine is an upper limit based on 2% detection limit for the undetected adenosine C-8 adduct and the observed  $k_{\text{nuc}}$  for formation of the benzene imine adducts **11a,b** (○).

2.3. This may be the approximate diffusion limit for these neutral–cation combination reactions since  $k_{\text{az}}$  for the cation–anion combination of **3a,b** with  $\text{N}_3^-$  under these conditions are apparently diffusion-limited at  $5.1 \times 10^9$  and  $5.0 \times 10^9 \text{ M}^{-1} \text{ s}^{-1}$ , respectively.<sup>14</sup> For  $\text{pK}_a \leq 2.3$ , log  $k_{\text{nuc}}$  varies with  $\text{pK}_a$  with a slope,  $\beta_{\text{nuc}}$ , of 0.7, so reactions that proceed with  $k_{\text{nuc}} < 2 \times 10^9 \text{ M}^{-1} \text{ s}^{-1}$  show significant dependence on the  $\text{pK}_a$  of  $\text{N}^7\text{-H}^+$ . The  $\beta_{\text{nuc}}$  of ca. 0.7 are lower limits because the data points for A that strongly influence the slopes are upper limits for both cases.

The data in Table 3 show that  $\text{X}^-$  reacts with **3a,b** with rate constants similar to those observed for G, dG, and 8-MeG. The  $\text{pK}_a(\text{N}^7\text{-H}^+)$  for N-1 deprotonated X ( $\text{X}^-$ ) has not been measured, but it can be estimated to be ca. 2.1 on the basis of the effect of N-1 deprotonation on the  $\text{pK}_a$  of  $\text{N}^7\text{-H}^+$  for other purine nucleosides.<sup>18</sup> The high selectivity of  $\text{X}^-$  for **3a,b** to form C-8 adducts is then a consequence of the basicity of N-7 in  $\text{X}^-$ .

(17) Sigel, H.; Massoud, S. S.; Corfu, N. A. *J. Am. Chem. Soc.* **1994**, *116*, 2958–2971. Evans, F. E.; Sarma, R. H. *J. Mol. Biol.* **1974**, *89*, 249–253. Martin, R. B. *Acc. Chem. Res.* **1985**, *18*, 32–38. Lönnberg, H.; Vihanto, P. *Inorg. Chim. Acta* **1981**, *56*, 157–161. Rawitscher, M.; Sturtevant, J. J. *Am. Chem. Soc.* **1960**, *82*, 3739–3740. Jencks, W. P.; Regenstein, J. In *CRC Handbook of Biochemistry and Molecular Biology, Physical and Chemical Data*, 3rd ed.; Fasman, G. D., Ed.; CRC Press: Inc.; Cleveland, OH, 1975; Vol. 1, pp 305–352.

(18) Kim, S.-H.; Martin, R. B. *Inorg. Chim. Acta* **1984**, *91*, 19–24.

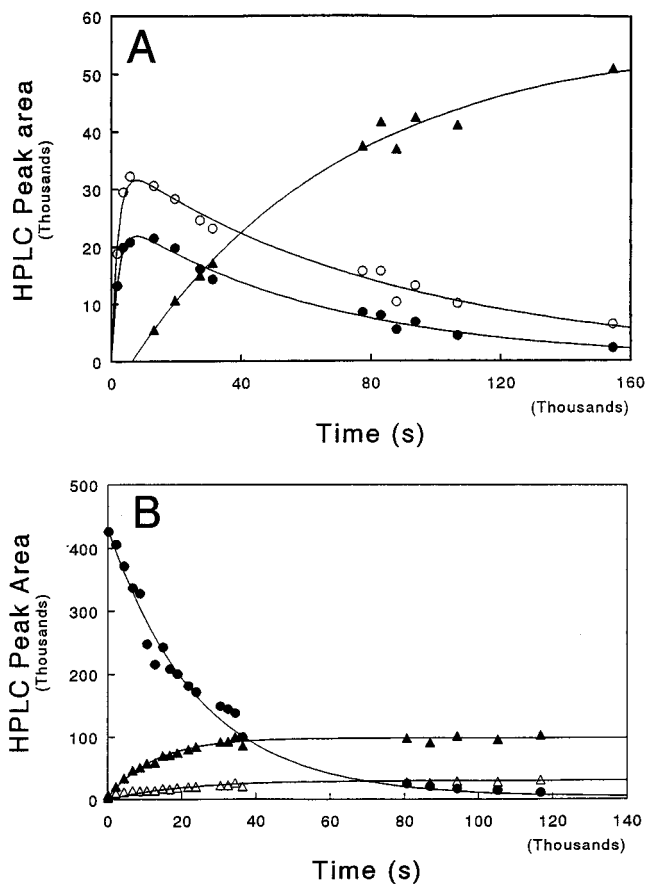
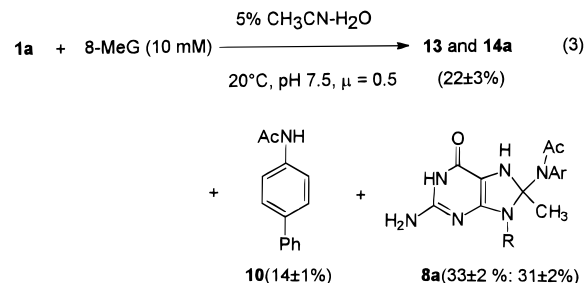


**Figure 8.** Time course for the appearance of products observed in the reaction of 8-MeG (10 mM) with **1a** (A) and **1b** (B) at pH 7.5. Data were fit to a standard first-order equation or to an equation for two consecutive first-order processes. (A) Two diastereomers of **16a** (○,  $k_1 = (5.1 \pm 0.5) \times 10^{-4} \text{ s}^{-1}$  and  $k_2 = (1.14 \pm 0.07) \times 10^{-5} \text{ s}^{-1}$ ; ●,  $k_1 = (4.5 \pm 0.4) \times 10^{-4} \text{ s}^{-1}$  and  $k_2 = (1.55 \pm 0.09) \times 10^{-5} \text{ s}^{-1}$ ) and the combined HPLC peak for both diastereomers of **8a** (▲,  $k_2 = (1.5 \pm 0.3) \times 10^{-5} \text{ s}^{-1}$ ). (B) Combined HPLC peak for the two diastereomers of **16b** (●), **10** (△), and the combined HPLC peak for the two diastereomers of **8b** (▲). First-order rate constants for the appearance or disappearance of these products are given in the text.

**8-Methylguanosine Reactions.** The reactions of **1a,b** with 8-MeG are unique because the final adducts **8a,b** are not produced at the same rate that **1b** decompose. In both cases, intermediate products are generated and subsequently converted into the final isolated adducts.

In 10 mM 8-MeG at pH 7.5, **1a** decomposes to yield the hydrolysis products **13** and **14a** ( $22 \pm 3\%$  combined yield), *N*-acetyl-4-aminobiphenyl (**10**,  $14 \pm 2\%$ ), and the two diastereomers of **8a** ( $33 \pm 2\%$  and  $31 \pm 2\%$ ) (eq 3). Figure 8A shows



that two intermediates are formed rapidly as **1a** decomposes in the presence of 8-MeG and that both of them subsequently decompose slowly. As they decompose the two diastereomers of **8a** are formed. Under the HPLC conditions employed here

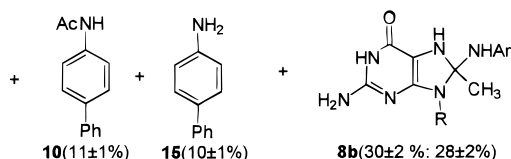
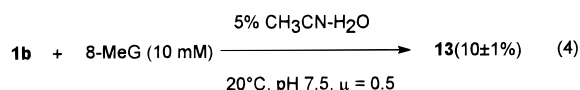
**Table 4.** NMR Data for the Two Intermediates (**16**) Observed at Early Reaction Times in the Reaction of **1b** and 8-MeG<sup>a</sup>

	<sup>1</sup> H resonances (ppm)	multiplicity, no. of H	<i>J</i> (Hz)	COSY correlation (ppm)
intermediate 1	6.78	d, 2H	8.5	7.46
	7.46	d, 2H	8.2	6.78
intermediate 2	6.74	d, 2H	8.5	7.44
	7.44	d, 2H	7.9 <sup>b</sup>	6.67

<sup>a</sup> One additional resonance at 2.45 ppm (3H, s) appears to be associated with these signals. This peak is very close to the C<sup>8</sup>-CH<sub>3</sub> resonance for 8-MeG, so the second expected methyl resonance for the intermediates is likely to be obscured. <sup>b</sup> This peak was partially obscured, so measurement of *J* was difficult. COSY correlations were unequivocal, however.

the two diastereomers of **8a** elute as a single peak. The rate constants for the appearance and disappearance of the intermediates are  $(5.1 \pm 0.5) \times 10^{-4}$  and  $(1.14 \pm 0.07) \times 10^{-5} \text{ s}^{-1}$ , respectively, for one and  $(4.5 \pm 0.4) \times 10^{-4}$  and  $(1.55 \pm 0.09) \times 10^{-5} \text{ s}^{-1}$ , respectively, for the other. The larger rate constants are very similar to the rate constant for hydrolysis of **1a** under these conditions of  $(4.0 \pm 0.5) \times 10^{-4} \text{ s}^{-1}$ . The calculated rate constant for the appearance of the **8a** diastereomers is  $(1.5 \pm 0.3) \times 10^{-5} \text{ s}^{-1}$ . This rate constant was calculated using data taken after  $10^4 \text{ s}$ , ca. 6 half-lives of the faster process. Figure 8A shows that the  $t = 0$  intercept for the first-order fit is quite negative, implying that there is an induction period for the formation of **8a**. These results show that the **8a** diastereomers are the products of the decomposition of the two intermediates. Since the amide **10** is a product of the slow decomposition of **8a**, we did not examine the time course for its appearance in detail, but it was clear that most of **10** produced in the first  $10^5 \text{ s}$  of this reaction did not result from decomposition of **8a**.

In 10 mM 8-MeG at pH 7.5, **1b** shows behavior similar to that of **1a**. Decomposition products included the hydrolysis product **13** ( $10 \pm 1\%$ ) and 4-aminobiphenyl (**15**,  $10 \pm 1\%$ ), **10** ( $11 \pm 1\%$ ), and the two diastereomers of **8b** ( $30 \pm 2\%$  and  $29 \pm 2\%$ ) (eq 4). All products except **13** are generated consider-

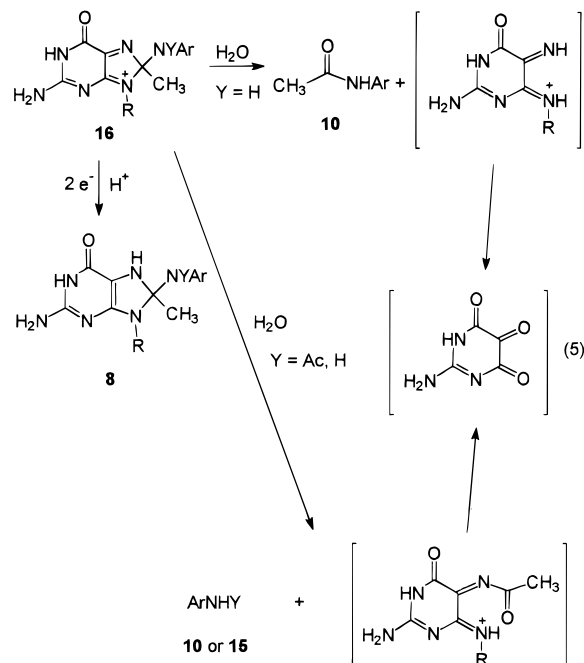


ably more slowly than the rate at which **1b** decomposes (Figure 8B). Their appearance is correlated with the disappearance of a single HPLC peak. Although only one HPLC peak was observed, <sup>1</sup>H NMR data taken at early reaction times at 0 °C indicate that there are two intermediates which decompose into the final products at comparable rates. Because of considerable peak overlap with the excess 8-MeG used in the NMR experiment, it was possible to obtain clear signals only for the amino-substituted aromatic ring of the biphenyl systems for both intermediates. These data are summarized in Table 4. The data indicate that this ring is not substituted on any of the original tertiary carbons of the ring and that the two intermediates are very similar in structure, apparently diastereomers.

The HPLC data of Figure 8B were fit to first-order rate equations to obtain rate constants of  $(4.1 \pm 0.3) \times 10^{-5} \text{ s}^{-1}$  for the disappearance of the peak for the intermediates,  $(4.9 \pm 0.6) \times 10^{-5} \text{ s}^{-1}$  for the appearance of the peak for **10**, and  $(8.0 \pm$

$0.8) \times 10^{-5} \text{ s}^{-1}$  for the appearance of the HPLC peak for the two diastereomers of **8b**. These rate constants are in good agreement considering that two of the HPLC peaks monitored are actually combined peaks for diastereomers that may decompose or appear at somewhat different rates.

The observations that the reaction of both **1a,b** with 8-MeG leads to two intermediates that give rise to the products indicated above and that the NMR data indicate that they have intact biphenyl ring systems suggest that these intermediates have the structures **16a,b**. Those intermediates should exist as a pair of diastereomers and their hydrolysis reactions could lead to **10** or **15** (eq 5). The likely byproducts of such reactions (eq 5)



have not been detected and would be difficult to find in the presence of excess 8-MeG. The observed adducts **8a,b** can be derived from **16a,b** by a  $2e^-$  reduction (eq 5). The likely source of reducing equivalents is the excess 8-MeG present during these experiments. Cyclic voltammetry confirms that 8-MeG has irreversible oxidation potentials at 0.64, 0.84, and 1.08 V vs an Ag/AgCl reference electrode.

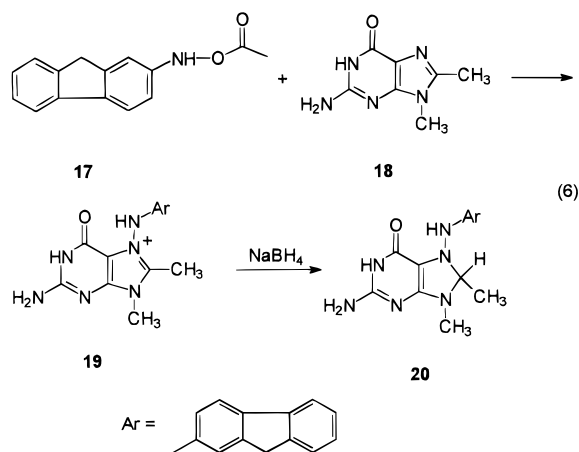
## Discussion

**Reaction Mechanisms.** All the purine nucleosides react with **1a,b** to form adducts, but not always C-8 adducts. In particular, I forms significant quantities of both C-8 and O-6 adducts, **6** and **7**, and A produces only the unique benzene imine derivatives, **11**. The dihydropurine derivatives, **8**, formed from the reaction of **1a,b** with 8-MeG appear to be reduction products derived from **16**. The reactions of 8-MeG appear to mimic those of dG, G, and the other nucleosides that produce C-8 adducts and also provide some insight into how these reactions occur.

It is clear from the kinetic and product data (Tables 1 and 2 and Figures 6 and 8) that the nucleosides trap an intermediate produced after the rate-limiting steps of the hydrolysis reaction of **1a,b**. N<sub>3</sub><sup>-</sup> trapping studies of the hydrolysis reactions of **1a,b** and the very good agreement between  $k_{az}/k_s$  ratios determined from hydrolysis studies and those directly measured by LFP methods have established that both **1a,b** generate the highly selective nitrenium ions **3a,b** in aqueous solution.<sup>7,14</sup> Since the purine nucleosides do not trap the quinol imines **12a,b** (Figure 6), it appears that all of the nucleoside-carcinogen adducts discussed here are produced by trapping of the nitrenium ions.

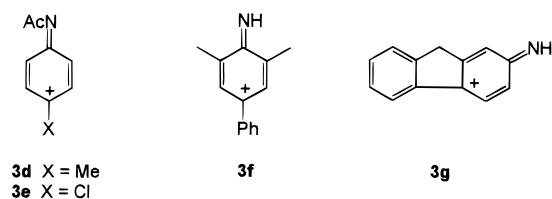


The C-8 adducts are of considerable interest because they are the predominant adducts reported from in vivo and in vitro studies,<sup>1,2</sup> so the detailed mechanism of this reaction has received some attention.<sup>1-4,19</sup> Several pieces of evidence indicate that the reaction occurs by initial attack of N-7 of the purine nucleoside on the N of the nitrenium ion. Kadlubar and co-workers have trapped the product of the reaction of *N*-acetoxy-2-aminofluorene (**17**) with *C*<sup>8</sup>,*N*<sup>9</sup>-dimethylguanine (**18**) by reduction with NaBH<sub>4</sub> and examined the initial product directly by NMR.<sup>4</sup> Their spectroscopic data are consistent with the structures **19** and **20** (eq 6).<sup>4</sup> They also examined the reaction



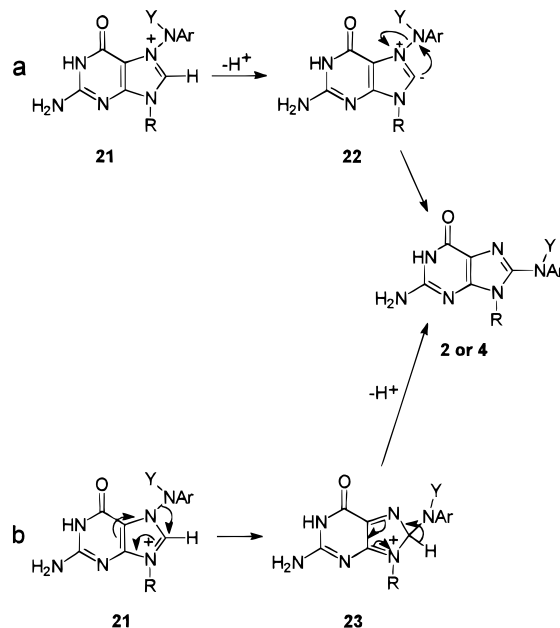
of **17** with 8-MeG and 8-Me-dG, but were not able to come to definite conclusion concerning adduct structures in those cases. On the basis of our results with **1a,b**, it is probable that they were observing adducts similar to **8** and/or **16** in those cases. Although nucleophilic attack on the N of the nitrenium ion is unusual, it is not unprecedented. We have shown that aniline and *N,N*-dimethylaniline trap the nitrenium ions **3a,c** in dry MeOH, in part, by nucleophilic attack on the N of both of these ions by either the amino group or C-4 of the aromatic amine.<sup>20</sup> Glutathione also attacks the N of the nitrenium ion.<sup>21</sup>

Our data show that for purine nucleosides with  $pK_a(N7-H^+)$  below ca. 2.3 the rate constant  $k_{nuc}$  for **3a,b** is below the diffusion limit and is strongly dependent on this  $pK_a$  with a  $\beta_{nuc}$  of at least 0.7 (Figure 7). These results are consistent with initial nucleophilic attack of N-7. These results also explain why dG and G are uniquely reactive with nitrenium ions to generate C-8 adducts. These nucleosides have the most basic N-7 sites of all the commonly occurring purine nucleosides, so they will have the most rapid reactions with nitrenium ions that react as selectively or more selectively than **3a**. Nitrenium ions less selective than **3a** may react with a wider range of purine nucleosides at the diffusion controlled limit, but these ions would also show overall reduced selectivity toward all nucleosides because of their rapid reactions with solvent. Indeed, we have been unable to detect any significant reactions of the less selective ions **3d,e** with purine nucleosides in an aqueous environment.<sup>22</sup>

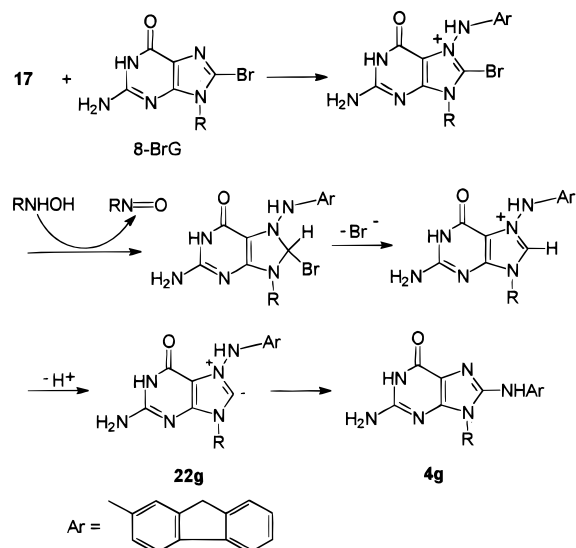


McClelland has shown that the nitrenium ion **3f** is quenched by dG with a rate constant of  $1.0 \times 10^8 \text{ M}^{-1} \text{ s}^{-1}$ .<sup>23</sup> This same

### Scheme 2



### Scheme 3



ion has a  $k_s$  of  $1.5 \times 10^5 \text{ s}^{-1}$ .<sup>23</sup> It is not known what the trapping product is in this case, but the quenching rate constant is about 1 order of magnitude smaller than that expected on the basis of comparisons to **3c** ( $k_s = 7.7 \times 10^4 \text{ s}^{-1}$ ,  $k_{dG} = 6.2 \times 10^8 \text{ M}^{-1} \text{ s}^{-1}$ ).<sup>3,14a</sup> This is consistent with moderate steric hindrance to nucleophilic attack on the nitrogen of the cation provided by the flanking methyl groups. Although it appears that the initial attack results in an intermediate of structure **21** (Scheme 2), subsequent steps resulting in the final C-8 adduct have not been clear. Kadlubar and co-workers favored mechanism a of Scheme 2 primarily on the basis of the isolation of a low yield (4%) of **4g** from reaction of 8-bromoguanosine (8-BrG) with **17**.<sup>4</sup> They proposed that this reaction proceeded by the mechanism of Scheme 3 to generate the zwitterion **22g** and, finally, the observed product **4g**. The low yield of **4g** could have been derived from the reaction of the 2-fluorenylnitrenium ion (**3g**) with G present as a 0.1% impurity in the 8-BrG.<sup>4</sup> Under their reaction conditions (5 mM 8-BrG, 37 °C), the residual G present in solution would account for the entire yield of **4g** if  $k_G/k_s$  for **3g** is ca.  $8.0 \times 10^3 \text{ M}^{-1}$ . This is possible since  $k_{d-G}/k_s$  for **3c** is  $4.8 \times 10^3 \text{ M}^{-1}$  at 30 °C<sup>24</sup> and **3g** is a more selective

ion than **3c** toward  $\text{N}_3^-$  ( $k_{\text{az}}/k_s = 5.4 \times 10^4 \text{ M}^{-1}$  for **3c** and  $1.2 \times 10^5 \text{ M}^{-1}$  for **3g**).<sup>14b</sup> A linear extrapolation of a plot of  $\log(k_{\text{dG}}/k_s)$  vs  $\log k_s$  (not shown) for **3a–c** provides an estimate of  $k_{\text{dG}}/k_s$  for **3g** at 20 °C of  $1.6 \times 10^4 \text{ M}^{-1}$ . If the temperature dependence of  $k_{\text{dG}}/k_s$  is similar for **3c** and **3g**,  $k_{\text{dG}}/k_s$  for **3g** at 37 °C will be ca.  $8.6 \times 10^3 \text{ M}^{-1}$ . We conclude that the low yield of **4g** observed by Kadlubar and co-workers is likely due to trapping of **3g** by the small amount of G present under the reaction conditions.

Our results are consistent with mechanism b of Scheme 2. The adducts **8a,b** clearly show that deprotonation of  $\text{C}^8\text{--H}$  is not necessary for C-8 adducts to form. We have observed intermediates that lead to **8a,b**. Since HPLC (Figure 8B) and NMR (Table 4) data show that in each case there are two intermediates leading to the final adducts, the intermediates we observe are not consistent with structures similar to **19** that could not exist as a pair of diastereomers. Our data are consistent with the proposed structure **16**, the  $\text{C}^8\text{--CH}_3$  analogue of **23**. The hydrolysis products derived from the intermediates and the ultimate stable adducts, **8**, are also consistent with the proposed structures.

Kadlubar and co-workers did directly observe **19**.<sup>4</sup> This compound was stable enough for  $^1\text{H}$  NMR measurements to be made, but we see no sign of similar adducts building up to detectable levels in our experiments with 8-MeG and **1a** or **1b**. The most significant difference in the experimental conditions employed lies in the choice of the purine nucleophile. The reaction of nitrenium ion **3g** with  $\text{C}^8, \text{N}^9$ -dimethylguanine leads to **19**, in which the N-9 can stabilize the structure by a direct resonance interaction. If the  $\text{N}^9\text{--CH}_3$  of **19** is replaced by an electron-withdrawing ribofuranosyl moiety, this resonance interaction is significantly curtailed and the resulting intermediate would be much less stable. This difference in stabilization may be sufficient to prevent observation of analogous intermediates in our experiments. Despite our inability to directly detect such intermediates in the present study, it seems clear, based on the strong dependence of  $k_{\text{nuc}}$  on the  $\text{pK}_a$  of  $\text{N}^7\text{--H}^+$  and on the results of Kadlubar and co-workers,<sup>4</sup> that the intermediates **21** (Scheme 2) are involved in these reactions.

**Site Selectivity.** For the more basic nucleosides, G, dG, 8-MeG, and  $\text{X}^-$ , reaction occurs exclusively at N-7 in aqueous solution, but as the basicity of N-7 decreases, the rate constant for trapping of nitrenium ions by N-7 decreases and other types of adducts are formed, specifically the O-6 adducts derived from I and the unique N-6 benzene imine adducts derived from A. Our data show that these are also formed as the result of nitrenium ion trapping (Figure 6). In these cases, the nucleophilic exocyclic O-6 or N-6 of the purines attack the nitrenium ion at the ortho or para carbons of the aromatic ring proximal to the nitrenium N. These are the normal sites of attack of typical hard nucleophiles such as  $\text{N}_3^-$  and  $\text{Cl}^-$ .<sup>7,25</sup>

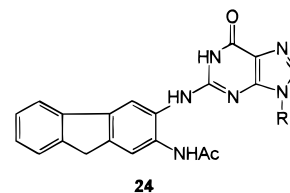
Only soft nucleophilic sites such as C,  $\text{S}^-$ , and neutral aromatic amines show any tendency to react with nitrenium ions at N, and even in these cases, a mixture of products is found

due to attack on both the aromatic ring and the N of the nitrenium ion.<sup>20,21</sup> The high selectivity of N-7 in basic purine nucleosides for N of the nitrenium ion is unprecedented and not fully understood. Steric effects may play some role in this selectivity since the initial product of N-7 attack on the ortho or para carbons of **3a–c** or **3g** would be quite sterically congested. Our data are in conflict with the recently published scheme of Dipple meant to explain site selectivity of the reactions of electrophilic carcinogens with purines.<sup>26</sup> In this scheme, hard electrophilic sites react at N-7 of G and A and soft electrophilic sites tend to react at N-2 and O-6 of G and N-6 of A.<sup>26</sup> Our data show the opposite selectivity for reactions of purines with *N*-arylnitrenium ions. A general pattern of site selectivity that can be applied across a wide range of electrophilic carcinogens is not yet apparent.

The pattern that emerges from this study and others<sup>3,4</sup> is that purine nucleosides containing a basic N-7 ( $\text{pK}_a$  of  $\text{N}^7\text{--H}^+ \geq 2.3$ ) react preferentially and selectively with long-lived nitrenium ions ( $1/k_s \geq 1.5 \times 10^{-7} \text{ s}$ ) to form an N-7 adduct **21** that subsequently undergoes rearrangement via mechanism b of Scheme 2 to form the C-8 adducts. This reaction is not competitive with solvent trapping of the ion for nitrenium ions with significantly shorter lifetimes ( $1/k_s < 5 \times 10^{-9} \text{ s}$ ) under accessible nucleoside concentrations ( $< 50 \text{ mM}$ ) because the diffusion limit for the nucleoside trapping reaction appears to be about  $2 \times 10^9 \text{ M}^{-1} \text{ s}^{-1}$ .

If the N-7 site of the purine nucleoside is less basic, alternative nucleophilic sites on the purine can compete with N-7 to form adducts of different structure. None of these reactions approach the selectivity observed for purine nucleosides with a basic N-7.

**Implications with Respect to Carcinogenesis.** Our data show why the major in vivo and in vitro DNA adducts of carcinogens such as **1a–c** and **17** are C-8 adducts formed at the dG base sites.<sup>1,27</sup> The N-7 of the dG moiety is the most reactive purine or pyrimidine base site toward nitrenium ions on DNA, and the initial N-7 adduct rearranges to form the observed C-8 adduct. The structure of the DNA does play some role in the site selectivity of nitrenium ions, however. Treatment of native DNA in vivo or in vitro with **1c** or its precursors leads to the formation of a minor (5–20% compared to C-8 adducts) N-2 adduct, **24**.<sup>1a–c,27</sup> A similar material is also observed as a



minor product of the reaction of 4-aminobiphenyl-derived carcinogens with native DNA.<sup>28</sup> This type of adduct is not observed in solution studies with dG, G, or denatured DNA,<sup>1d,2,3</sup> so its formation must be a consequence of the modification of the site selectivity of the nitrenium ion by the three-dimensional structure of duplex DNA.

Although the structure-induced modification of nitrenium ion site selectivity may have a relatively minor effect on product distributions, it can have a major effect on the physiological role of the carcinogen. For example, the N-acylated C-8 adducts are subject to relatively efficient excision and repair, but the N-2 adduct is much more persistent in vivo and, for that reason,

(19) Miller, J. A.; Miller, E. C. *Environ. Health Perspect.* **1983**, *49*, 3–12. Garner, R. C.; Martin, C. N.; Clayson, D. B. In *Chemical Carcinogens*, 2nd ed.; Searle, C. E., Ed.; ACS Monograph 182; American Chemical Society: Washington, DC, 1984; Vol. 1, pp 175–276.

(20) Novak, M.; Rangappa, K. S. *J. Org. Chem.* **1992**, *57*, 1285–1290. Novak, M.; Rangappa, K. S.; Manitsas, R. K. *J. Org. Chem.* **1993**, *58*, 7813–7821.

(21) Novak, M.; Lin, J. *J. Am. Chem. Soc.* **1996**, *118*, 1302–1308.

(22) Novak, M.; Pelecanou, M. Unpublished results.

(23) McClelland, R. A. Personal communication.

(24) Novak, M.; Kennedy, S. A. *J. Phys. Org. Chem.* **1997**, in press.

(25) Novak, M.; Kahley, M. J.; Lin, J.; Kennedy, S. A.; Swanegan, L. *J. Am. Chem. Soc.* **1995**, *117*, 574–575. Novak, M.; Kahley, M. J.; Lin, J.; Kennedy, S. A.; James, T. G. *J. Org. Chem.* **1995**, *60*, 8294–8304.

(26) Dipple, A. *Carcinogenesis* **1995**, *16*, 437–441.

(27) Kriek, E. *Cancer Res.* **1972**, *32*, 2042–2048. Westra, J. G.; Kriek, E.; Hittenhausen, H. *Chem.-Biol. Interact.* **1976**, *15*, 149–164.

(28) Kriek, E.; Hengeveld, G. M. *Chem.-Biol. Interact.* **1978**, *21*, 179–201.

may be ultimately more important to carcinogenesis than the more abundant N-acylated C-8 adducts.<sup>1a-e,27</sup> We are currently examining the effects of DNA structure on the efficiency of nitrenium ion trapping by dG residues.<sup>24</sup>

**Acknowledgment.** This work was supported by a grant from the American Cancer Society (CN-23K). The 300 MHz <sup>1</sup>H and 75.5 MHz <sup>13</sup>C NMR spectra were obtained with equipment funded by NSF Grant No. CHE9012532. The LD-TOF mass spectra were obtained at Miami on equipment funded by the NSF-ARI program (CHE-9413529) and the Ohio Board of Regents Action Fund. Other mass spectra were obtained at The Ohio State University Chemical Instrumentation Center. We

thank Dr. Carolyn Cassady for help with interpretation of FAB and LD-TOF mass spectra. We also thank Dr. Robert A. McClelland for sharing preliminary data with us and for helpful discussions.

**Supporting Information Available:** Isolation and characterization of nucleoside–carcinogen adducts, COSY and XH-CORR correlation tables for adducts **5–8** and **11**, trapping data for **1a,b** with various nucleosides, and plot of observed  $k_x/k_s$  vs pH for **1b** (21 pages). See any current masthead page for ordering and Internet access instructions.

JA970698P